

Validation of GEANT4 for Accurate Modeling of ^{111}In SPECT Acquisition

Bernd Schweizer, Andreas Goedicke

Philips Technology Research Laboratories, Aachen, Germany
bernd.schweizer@philips.com

Abstract. Quantitative SPECT imaging of ^{111}In is of growing importance in nuclear medicine applications like patient-specific radionuclide dosimetry. In this study, the quality of a Monte-Carlo based model of the imaging chain from nuclear decay to detection in a gamma camera is investigated. Important characteristics like the camera point spread function (PSF), the phantom attenuation and scatter effects are compared between simulation and experiment. The model shows a good agreement to the actual measurements and allows for further use in the development of quantitative SPECT reconstruction which will be mandatory for future oncology.

1 Introduction

Single Photon Emission Computed Tomography (SPECT) is an important nuclear imaging modality. In this study, imaging of ^{111}In is investigated, a radioisotope mainly used for applications in oncology. Here, the absolute assessment of local tracer activity provides access to both tumor viability staging and treatment prognosis. Due to its special characteristics including two equally dominant particle energy lines, ^{111}In imaging can become rather challenging in terms of image quality degradation e.g. due to down-scatter contamination. We present qualitative and quantitative comparisons between experimental and simulated gamma camera data acquisitions in order to prove the quality of a Monte-Carlo based imaging model to be used in the development of a next-generation quantitative SPECT reconstruction.

2 Materials and Methods

2.1 Phantom Acquisitions

Gamma camera acquisitions from two different phantom types have been acquired on a Philips Precedence SPECT/CT scanner at Rigs Hospital in Copenhagen. For PSF assessment, a planar measurement with a point source realized as an activity of 7.4 MBq ^{111}In located in a syringe tip was used. For the evaluation of attenuation and scatter impact, a SPECT scan from a NEMA PET

phantom was acquired (Fig.1(a)). Two cylinders have been filled with different concentrations of ^{111}In diluted in water: the outer cylinder (9.3 kBq/cm^3 , "warm background") and one insert (88.2 kBq/cm^3 , "hot insert"). In addition to that, two "cold" cylinders (air and Teflon) have been installed. Applied ^{111}In activities were determined with a Capintec CRC-15R dose calibrator. Volume measures were derived by a segmentation procedure based on CT images of the phantom. For the point source measurement, a source-to-camera distance of 15 cm was chosen and $5 \cdot 10^5$ counts were detected in a planar configuration. For the NEMA PET phantom, 128 projections with $(128\text{ pixels})^2$ resolution on a circular trajectory have been measured (Fig.1(a)). The acquisition time per projection was 30 s. In all acquisitions, a standard MEGP collimator was used and a standard dual ^{111}In energy window setting has been chosen for energy discrimination (1: 154 – 188 keV, 2: 221 – 270 keV).

2.2 Monte-Carlo Simulations

For Monte-Carlo simulations of the imaging chain, an advanced SPECT simulation framework based on GEANT4 [1] has been used, which was accelerated via the Forced-Detection-based variance reduction technique [2][3]. As an input for the simulation, voxelized activity and attenuation maps for the different phantom parts as well as the patient table models have been generated from the acquired CT-scan data (Fig.1(b)). The camera model included a standard MEGP collimator as well as a 9.5 mm scintillator crystal plate of NaI. Post-processing of the simulated detector events was performed to emulate binning impact, signal blurring (light spread) and effects of the detector electronics. According to the activity in the experiment, the number of simulated photon histories per projection was $2.4 \cdot 10^9$ for the point source and $4.4 \cdot 10^9$ for the NEMA PET phantom.

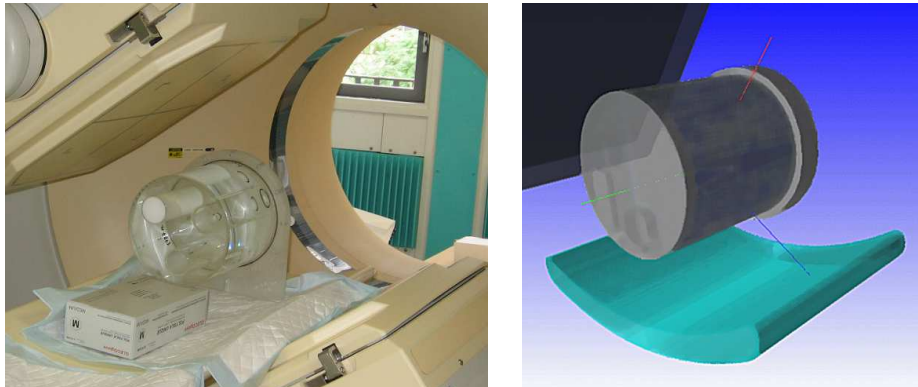


Fig. 1. Experimental setup for the NEMA PET phantom acquisition in the Philips Precedence SPECT/CT scanner (left). Modeling of the measurement in the GEANT4 based SPECT simulation framework (right).

2.3 Analysis

Planar gamma camera images of the point source were projected along pixel rows to obtain 2D profile plots of the PSF. The absolute camera sensitivity S was calculated from point-source images as $S = N/(A \cdot T)$, with N the number of detected counts, A the phantom activity and T the acquisition time. For the NEMA PET phantom, the detected counts in each projection were plotted against the projection number. The scatter fraction for each detection window was determined by applying a triple energy window (TEW) technique on the simulated projection data.

3 Results

The analysis of the PSF-profile plots (Fig.2) shows a good agreement between the experiment (red) and simulation of an idealized point source in air (green) with respect to signal intensity and shape in the central part of the curve. A further significant improvement, especially for the non-central areas was observed after including the patient tray and the camera lead shielding and plastic cover in the simulation (blue curve). The achieved improvement indicates that these signal components are due to additional scatter events from these parts of the simulation geometry. The remaining differences in the wing area of the curve can be explained by the basic strategy of the forced detection method to exclude those parts of the geometry from the radiation transport which generally only yield negligible contributions to the main result.

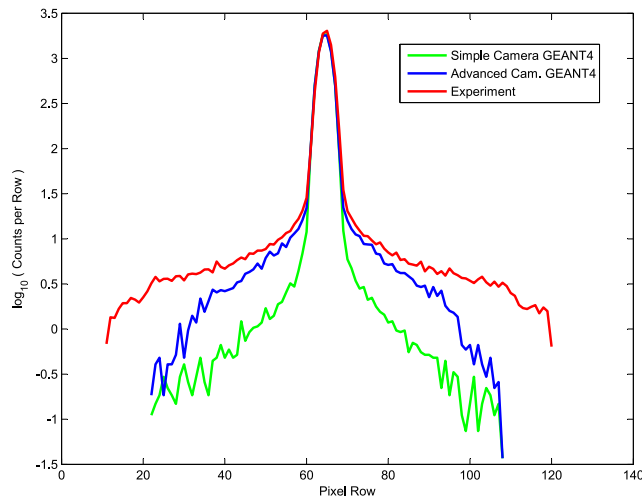


Fig. 2. Comparison between measured and simulated In-111 PSF on a logarithmic scale.

However, it should be noted that the signal level here is more than two orders of magnitude below the peak signal (and even lower, if the data is analyzed in the 2D detector area as opposed to a 1D-projection like in Fig.2). The agreement in the PSF amplitude is also reflected in the camera sensitivity figures, calculated

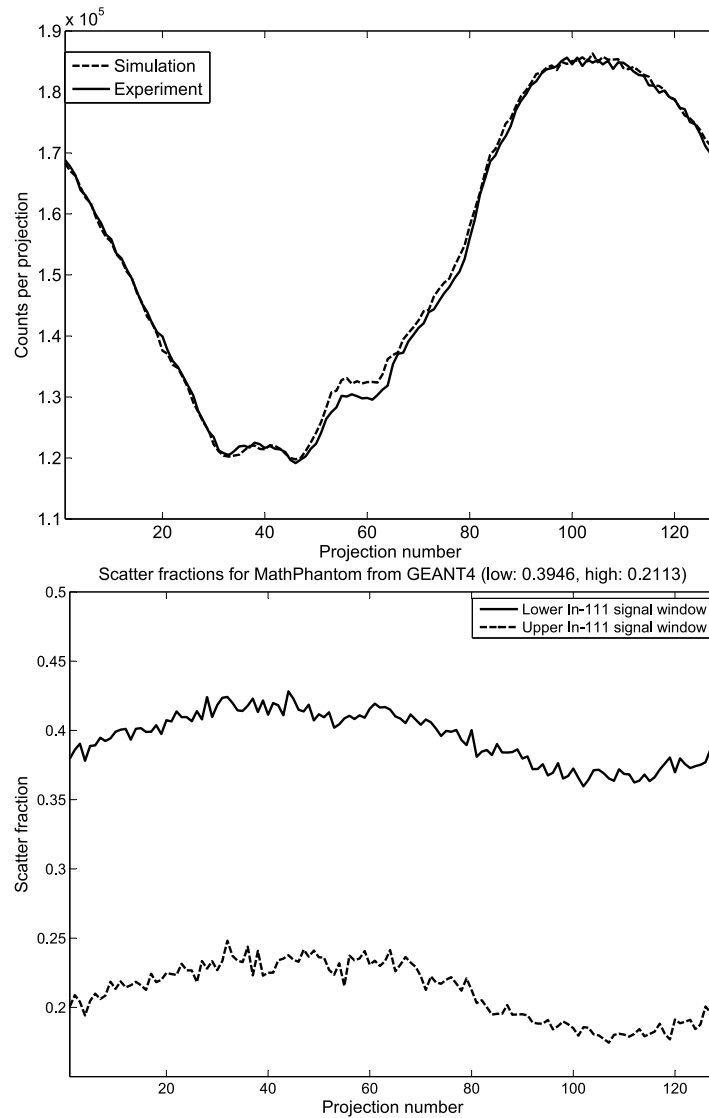


Fig. 3. Detected counts as a function of the camera angle for the NEMA PET phantom. Both curves are normalized to the same integral number of counts (top). Scatter fraction in lower and upper ^{111}In energy window as a function of the projection number for the NEMA PET phantom simulated in GEANT4 (bottom).

as $S = 163$ cps/MBq for the measured and 157 cps/MBq for the simulated point source acquisitions. In Fig.3(a), the detected counts per projection in the experiment and the simulation are compared with each other. Note that the focus of this analysis is on an analysis of the attenuation and scatter impact. Therefore the two curves were normalized to the same integral number of counts in order to facilitate the shape comparison. Obviously, the curves show an extremely good agreement. The determined integral difference between both plots before normalization was 6.9%, which is clearly within the boundaries of the experimental activity calibration error. In addition to that, Fig.3(b), displays the scatter fraction in the simulated signal for the NEMA PET phantom. The mean scatter fractions of 39.5% for the lower energy window and 21.1% for the upper energy window are in good agreement with other studies from literature [4], where for a similar approach values of 43% and 22% respectively are reported.

4 Discussion

The results achieved for both phantom types demonstrate a good agreement between experiment and simulation. In the PSF studies, the accurate modeling of important camera properties like PSF shape and absolute camera sensitivity could be demonstrated, especially when a realistic scanner model is included in the simulation geometry. This indicates that more complex phantom geometries can also be modeled accurately since such a case can be regarded as a superposition of point-sources from a mathematical view-point. In the NEMA PET phantom studies, detailed modeling of the complete imaging chain from nuclear decay to detection in the gamma camera could be proven. The quality of the Monte-Carlo simulation data warrants its use in quantitative SPECT. Future work based on these results will include the generation of highly realistic test datasets for algorithm development as well as use of accurate physical models in advanced SPECT reconstruction.

References

1. Agostinelli S, et al. GEANT4: a simulation toolkit. *Nucl Instrum Methods Phys Res A*. 2003;506:250–303.
2. de Jong HWAM, Beekman FJ, Slijpen TP. Acceleration of Monte Carlo SPECT simulation using convolution-based forced detection. *IEEE Nucl Sci Symp Conf Rec*. 1999 24-30 Oct;3:1532–6.
3. Goedicke A, Schweizer B, Staelens S, et al. Fast simulation of realistic SPECT projections using forced detection in GEANT4. In: *Proc Med Biol Eng Conf*; 2005.
4. Holstensson M. *Optimisation of Window Settings for Quantitative ^{111}In Imaging: A Comparison of Measurements to Monte Carlo*. Sweden: Lund University; 2006.